Current Journal of Applied Science and Technology

36(1): 1-8, 2019; Article no.CJAST.49566
ISSN: 2457-1024
(Past name: British Journal of Applied Science & Technology, Past ISSN: 2231-0843, NLM ID: 101664541)

SAR Calculations of Novel Dual-band PIFA for Mobile Phone Applications

Rasha Ali[1], M. I. Ahmed[2*], Walid S. El-Deeb[1] and A. A. Shaalan[3]

[1]Department of Electronics and Communication Engineering, Faculty of Engineering, University of Zagazig, Egypt.
[2]Department of Microstrip, Electronics Research Institute, Giza, Egypt.
[3]Department of Electronics and Computer Engineering, Faculty of Engineering, Delta University of Science and Technology, Egypt.

Authors' contributions

This work was carried out in collaboration among all authors. All authors read and approved the final manuscript.

Article Information

DOI: 10.9734/CJAST/2019/v36i130214
Editor(s):
(1) Dr. Chien-Jen Wang, Professor, Department of Electrical Engineering, National University of Tainan, Taiwan.
Reviewers:
(1) Joel Herrera, Clemson University, USA.
(2) P. Madhumathy, Dayananda Sagar Academy of Technology and Management, India.
(3) A. Ayeshamariam, Khadhir Mohideen College, India.
Complete Peer review History: http://www.sdiarticle3.com/review-history/49566

Original Research Article

Received 30 March 2019
Accepted 11 June 2019
Published 19 June 2019

ABSTRACT

Aims: The objective of this paper is to design a new PIFA for cell phone applications with low SAR.
Study Design: The designed PIFA antenna involves a patch with slots on the upper side of first substance layer FR-4, shorting wall, and a ground plane in the bottom side of second substance layer FR-4 and exciting (feeding port).
Place and Duration of Study: Department of Electronics and Communication Engineering, Faculty of Engineering, University of Zagazig. Between December 2017 to March 2019.
Methodology: it will be utilized SAM head model and a hand phantom as a user's head and hand. Time-domain solver considers hexahedral mesh with adaptive meshing scheme used in this simulation.
Results: The simulation result has been obtained using MWS CST tools which constructed on the finite integration technique. And the measurement results are accomplished with vector analyzer ZVA 67. The simulated and the investigational results are the same approximately.

**Corresponding author: E-mail: miahmed@eri.sci.eg;*

Conclusion: The antenna provides high gain for both frequency bands (900MHZ and 1800MHZ) with approximately 90% radiation efficiency. Moreover, The SAR analysis of the suggested antenna clearly demonstrates little SAR characteristics suitable for human usage competed with the standards of the safe SAR values.

Keywords: Planar inverted-F Antenna (PIFA); numerical specific anthropomorphic mannequin (SAM); electromagnetic (EM) and specific absorption rate (SAR).

1. INTRODUCTION

Mobile headphones have come to be necessary amongst all classes of people from kids to teenagers to adults all over the world. The significance of cell phones and their applications comes from providing the facility to retain in link with the surrounding world in a simple and up-to-date approach. With the advantages of cell phones, people typically forget the potential influence of the EM fields created by cellular headphones antennas' on the human brain.

Mobile proficiency is speedily rising. On average, at the finale of the year, 2022 mobile subscriptions worldwide will be more than 9 billion people [1]. Alongside this development, serious concerns about the EM radiation effects on human well-being [2]. During mobile, the call is a portion of EM radiation wave either engrossed or transmitted by the human head which in turn leads to heat effect on human tissue. The vital parameter that stated the quantity of power engrossed by the human tissue as exposed to (EM) radiation is (SAR).

Now a day's different types of multiband antennas are planned which can able to cover a number of operating frequency bands with close size. In [3,4] multi-loop –type antenna with a meander structure were exploited to accomplish compact size and multiband operations. With technological development, therefore the diversity of desires during this space are resulting in the creation of ever smaller, lighter, and additional multifunctional mobile handsets [5]. As a result, antennas have gone from external to internal; they need additionally become subject to varied constraints in size and performance. The planate inverted-F antenna (PIFA) is to satisfy the necessities of the present market.

With these developments, cellular headphones antennas have been transformed from single-band to multi-band characteristics [6-7]. In [8] a tetra brand planar inverted-F antenna (PIFA) for mobile handset applications is planned and meander line is exploited in reduction the antenna size. In [9] slot size modification and the inset-feed point are utilized to accomplish dual-band property.

Researchers are prepared to shrink SAR value. Various means were functioned to shrink the SAR created by a handset antenna definitely over the last years, the electromagnetic band-gap (EBG) secondary antenna elements, ferrite loading, meta-materials, and artificial magnetic conductors (AMC). Authors in [10] combined metamaterial configurations positioned between single-band (PIFA) and the human head and the SAR is condensed by 53% for 1 g tissue mass. In [11], the reduction of SAR is done by leading a U-edge wall made of an engrossing water material at each corner of the ground plane. In [12], the mobile antenna is intended to decrease antenna radiation towards the human body using the vertical sidewalls to blockade the radiation to the human body.

2. ANTENNA DESIGN

The architecture of the recommended PIFA is publicized in Fig. 1 which functioned at 900 MHz and 1800 MHz. It consists of two FR-4 substance with dielectric constant 4.4, loss tangent = 0.02 and thickness = 0.8 mm separated by foam. the ground (GND) found on the bottom surface of the first substance and has a dimension of 100 mm length and 40 mm width and it is connected with the top patch elements using a shorting wall with dimension 6.8 mm × 2.3 mm × 0.5 mm. Fig. 1 shows in details the geometry of the printed patch with slots as seen from above. The antenna takes up an area occupying 40 x 22 mm^2 on the upper surface of the second FR-4substance. The patch is placed at a height h=6.8 mm from the horizontal plane of the ground plane. The intended structure is excited with a coaxial feed of input impedance (Z_0= 50 ohms).

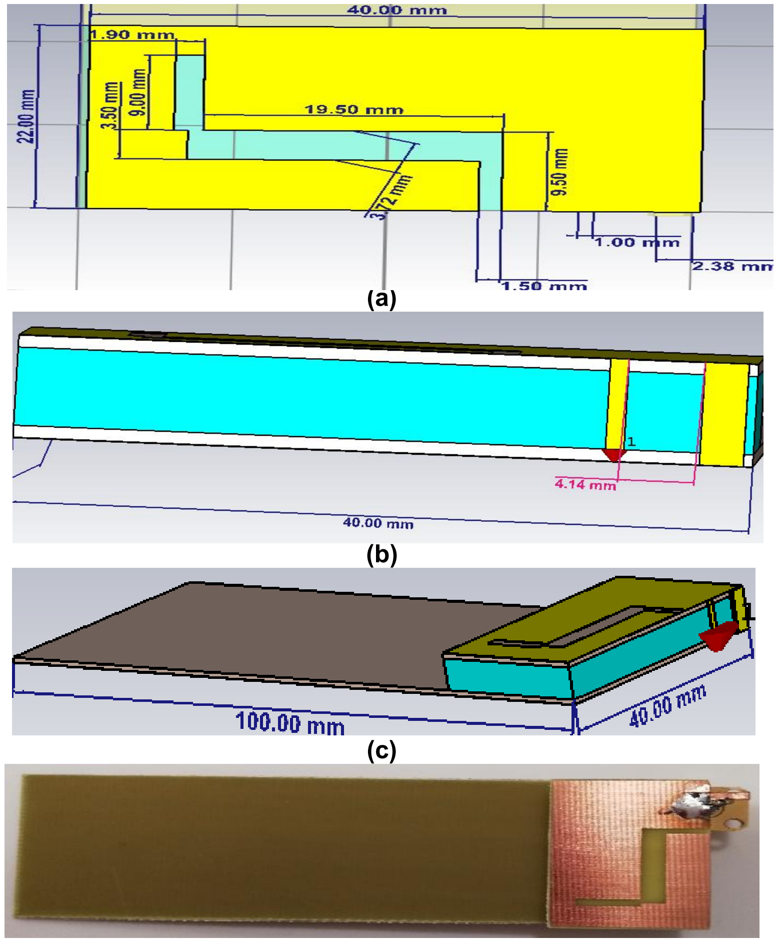

(a)

(b)

(c)

(d)

Fig. 1. Antenna geometry. (a) Upper vision, (b) side vision, (c) Intended antenna and (d) photo of the fabricated antenna

The PIFA is manufactured by referring the design model in the CST microwave software as exposed in Fig. 1c To confirm the simulation outcome is exactly the same as the measurement outcome those copper plates and ground planes must be measured the same as the model design in order.

3. METHODOLOGY AND MODELS

The human insulator properties of tissues will be set into considerations to decide the contact between EM sources and the cell handset. In this letter, it will be utilized SAM head model [13] and a hand phantom as a user's head and hand. The SAM phantom has a shell and simulating liquid. The international standard organization [14-15] define SAM phantom insulator properties constructed on insulators properties, such as permittivity and conductivity of human tissues.

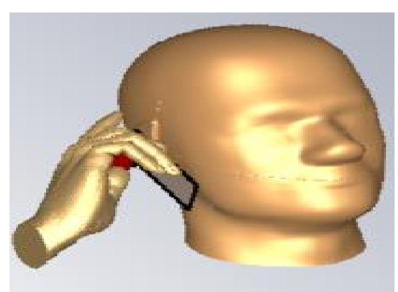

Fig. 2. Mobile antenna with a head hand model

We take into consideration the permittivity and conductivity of human tissues which are frequency determined parameters [16], and the respective values are constructed on human tissue measurement data as labeled in [17-18]. Table 1 indicates the insulator properties of head and hand phantom for dissimilar frequencies.

Time-domain solver considers hexahedral mesh with adaptive meshing scheme used in this simulation. Fig. 2 explains the configuration of the mobile antenna with head hand model. The generated electric field (E) in the human biological tissue can be developed to evaluate the engrossed power. Formula (1) and (2) are spent to compute total power absorbed and SAR correspondingly [19-20].

$$P_{abs} = 1/2 \int_V \sigma|E|^2 dV \quad (1)$$

$$SAR = \frac{\sigma|E|^2}{2\rho} \quad (2)$$

where E = electrical field, σ = tissue conductivity and ρ = tissue mass density.

4. SIMULATED AND MEASURED RESULTS

The measurement process is accomplished with vector network analyzer ZVA 67 to authorize that the resulting waveform is equivalent to the result obtained from the simulation process. Fig. 3 and Fig. 4 displays the antenna under test setup.

The radiated pattern is measured in the anechoic chamber as revealed in Fig. 4. The results are organized into two quantities which are simulation results of PIFA antenna and measurement results. S11 characterizes the quantity of the power which reflected from the antenna and therefore is identified as the return loss. The good functioning of the antenna should indicate a return loss of fewer than -10 dB. Fig. 5 expresses the results of reflection coefficient from simulation and measurements which have a little different in the frequency but it still in the limit of mobile applications.

One of the most significant factors of the antenna that designate the antenna's capability to direct the input power into radiation in a convinced direction is the gain. Built on Table 2 . the gain values of the intended antenna are (2.1 dB & 4 dB) for 900 MHz and 1800 MHz, correspondingly. Fig. 6 and Fig. 7 demonstrate the radiation pattern results from simulation and measurements for the intended antenna which specifies that they are similar and suitable for mobile communication terminals.

Table 1. Insulator properties of head and hand phantom

Frequency (MHZ)	Relative permittivity, εr			Conductivity, σ (S/m)		
	Shell	liquid	hand	Shell	liquid	hand
900	3.7	40.5	36.2	0.0016	0.97	0.79
1800	3.5	39	32.6	0.006	1.4	1.26

Table 2. The gain of the intended antenna

Frequency(MHZ)	900	1800
Simulated	2.1	4
Measured	1.9	3.8

Table 3. The max-average SAR_{1g} values for the suggested antenna in various distance from 7mm to 22 mm (SAR<1.6w/kg)

Resonance frequency(MHZ)	SAR (W/Kg)			
	7mm	12mm	17mm	22mm
900	1.256	1.034	0.846	0.6846
1800	1.383	0.7171	0.4299	0.2832

Table 4. The max-average SAR_{10g} values for the suggested antenna in various distance from 7mm to 22 mm (SAR<2w/kg)

Resonance frequency(MHZ)	SAR (W/Kg)			
	7mm	12mm	17mm	22mm
900	0.867	0.7222	0.5982	0.4884
1800	0.7304	0.3982	0.2472	0.183

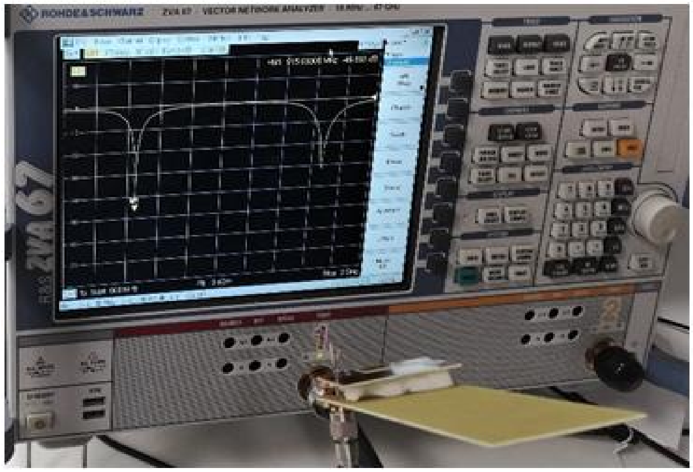

Fig. 3. Return loss measurement

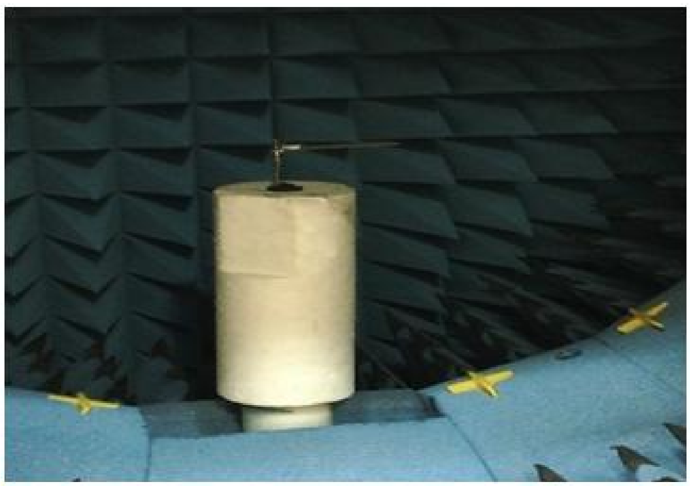

Fig. 4. Radiation pattern measurement

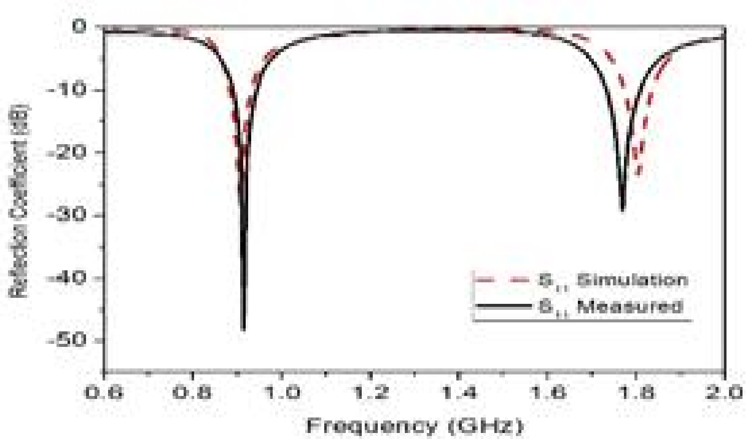

Fig. 5. Return loss of designed antenna(simulation & measurement)

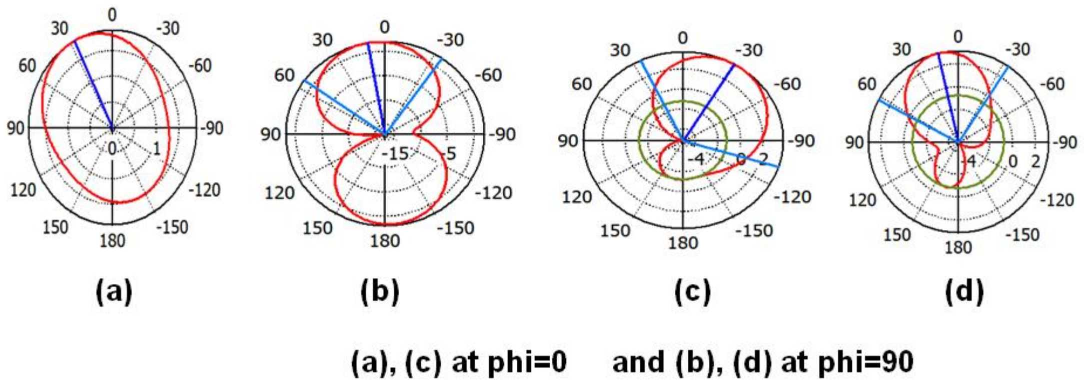

Fig. 6. Simulated radiation pattern: (a), (b) at 900 MHz, (c), (d) at 1800 MHz

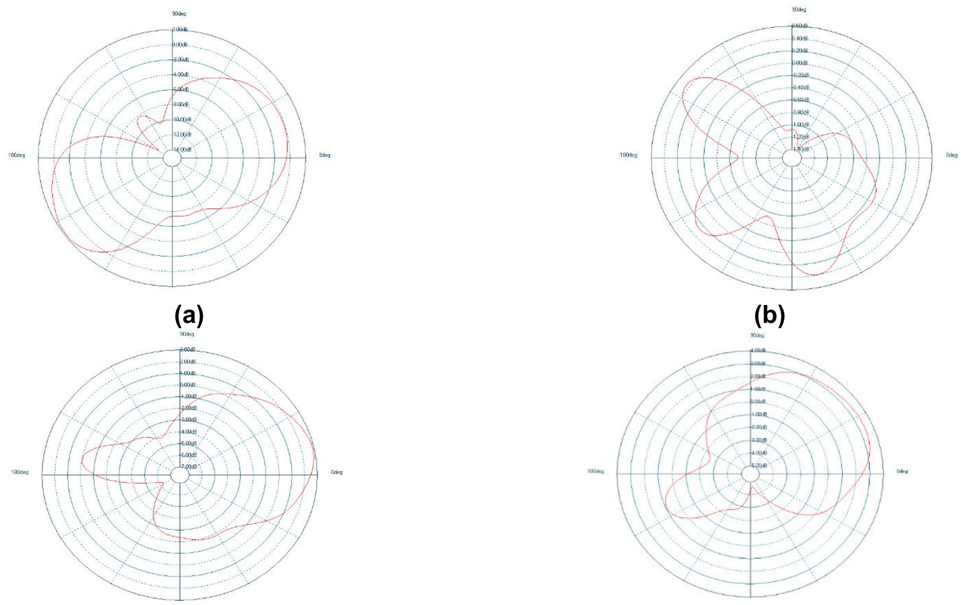

(a) (b)

(c) (d)

(a), (c) at phi=0 (b), (d) at phi 90

Fig. 7. Measured radiation pattern: (a), (b) at 900 MHz, (c), (d) at 1800 MHz

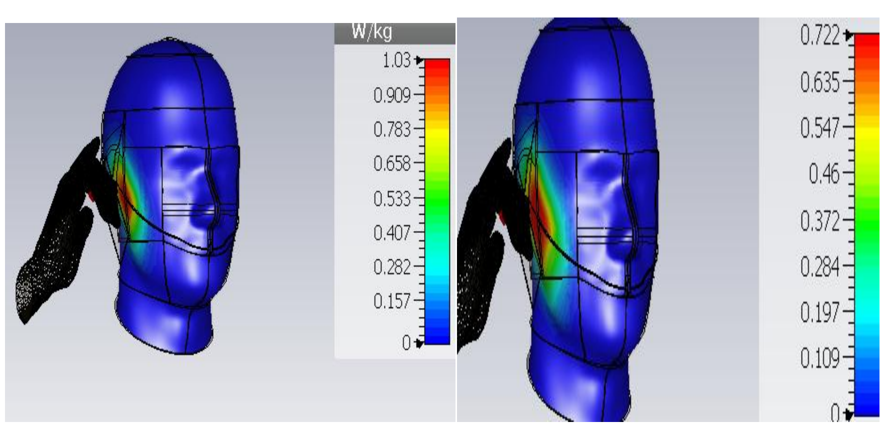

(a) (b)

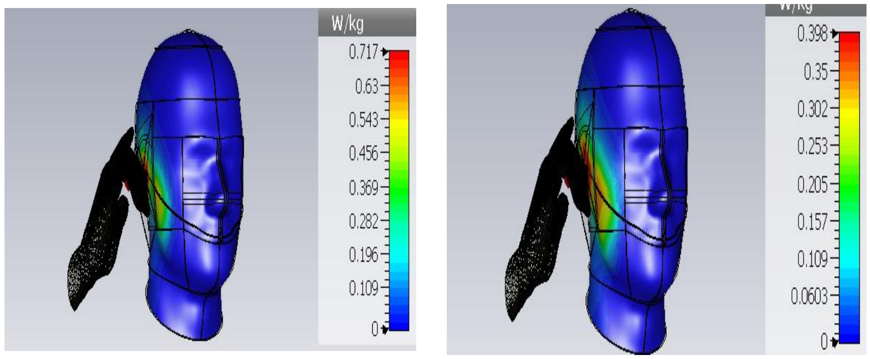

(c) (d)

Fig. 8. SAR distribution at distance 12 mm from the antenna: (a) f =900 MHz (1g), (b) f=900 MHz (10g), (c) f =1800 MHz, (1g) and (d) f=1800 MHz (10g)

Table 5. SAR values at distance 12mm from the antenna for various frequencies in the band

SAR(W/KG)	Frequency (MHZ)			
	892	930	1771	1833
1g	0.893	1.533	0.632	0.7765
10g	0.6235	1.066	0.3517	0.4278

5. SAR CALCULATIONS

"The SAR limit stated in IEEE C95.1: 2005 has been apprised to 2 W/kg over any 10 g of tissue, which is comparable to the limit stated in the International Commission on Non-Ionizing Radiation Protection (ICNIRP) guidelines" [21]. The average SAR values over (1 g and 10 g) were calculated in the post possessing phase of simulation affording to the IEEE standard algorithm [22] by setting excitation equal to 500 mW. Fig. 8 displays SAR distribution at distance 12 mm from the antenna that illustrates the results are suitable according to standards.

From Table 3 and Table 4, the small SAR value at the resonance frequencies has been observed to meet the international safety standards (FCC & ICNIPR) (1 g &10 g). Table 5 demonstrate SAR (1 g &10 g) values at 12 mm from the antenna at different frequencies.

6. CONCLUSION

A novel dual-band low SAR PIFA is planned for GSM and DCS bands applications. The antenna provides high gain for both frequency bands with approximately 90% radiation efficiency. Moreover, The SAR analysis of the suggested antenna clearly demonstrates little SAR characteristics suitable for human usage competed with the standards of the safe SAR values. The antenna was executed using the CST simulator and manufactured using the photolithographic technique. The simulated and the investigational results are the same approximately.

COMPETING INTERESTS

Authors have declared that no competing interests exist.

REFERENCES

1. Available:https://www.ericsson.com/en/mobility-report.
2. Lavanya A. Bhanu. Effects of electro-magnetic radiation on biological systems: A short review of case studies. In 8th international conference on electro-magnetic interference and compatibility, IEEE. 2003;87-90.
3. Chu FH, Wong KL. Internal coupled-fed dual-loop antenna integrated with a USB connector for WWAN/LTE mobile handset. IEEE Trans. Antennas Propag. 2011;59: 4215–4221.
4. Chen WS, Jhang WC. A planar WWAN/LTE antenna for portable devices, IEEE Antennas Wirel. Propag. Lett. 2013; 12:19–22.
5. Bhatti RA, Pack SO. Hepta-band internal antenna for personal communication handsets. IEEE Trans. Antennas Propag. 2007;55(12):3398–3403.

6. Yao Y, Wang X, Chen X, Yu J, Liu S. Novel diversity/MIMO PIFA antenna with broadband circular polarization for multimode satellite navigation. Antennas Wirel. Propag. Lett. IEEE. 2012;11:65–68.
7. Secmen M. Multiband and wideband antennas for mobile communication systems. Recent Dev. Mob. Commun.-Multidiscip. Approach; 2011.
8. Tarbouch M, El Amri A, Terchoune H. Design, realization and measurements of compact tetraband PIFA antenna for mobile handset applications. Journal of Engineering Technology. 2017;6(1):59-71. (ISSN: 0747-9964)
9. Rambe AH, Abdillah K. A low profile rectangular patch microstrip antenna for dual-band operation of wireless communication system. In IOP Conference Series: Materials Science and Engineering. IOP Publishing. 2018;309(1):012046.
10. Faruque MRI, Islam MT, Ali MAM. (A new design of metamaterials for SAR reduction. Measurement Science Review. 2013;13(2):70-74.
11. Nasser N, Serhal D, Barake R, Rammal M, Vaudon P. A novel low SAR water-based mobile handset antenna. Analog Integrated Circuits and Signal Processing. 2018;96(2):353-361.
12. Kusuma AH, Sheta AF, Elshafiey I, Alkanhal M, Aldosari S, Alshebeili SA. Low SAR antenna design for modern wireless mobile terminals. In STS International Conference; 2010.
13. Faruque MRI, Islam MT, Misran N. Analysis of electromagnetic absorption in mobile phones using metamaterials. Electromagnetics. 2011;31(3):215–232.
14. EC 106/61/CDV. Methods for the assessment of electric, magnetic and electromagnetic field associated with human exposure. Committee Draft for Voting; 2003.
15. CENELEC. Product standard to demonstrate the compliance of mobile phones with the basic restrictions related to human exposure to electromagnetic fields (300 MHz to 3 GHz). Ref. No. EN 50360:2001; 2001.
16. Hossain MI, Faruque MRI, Islam MT. Low SAR microstrip patch antenna for mobile phone. Frequenz. 2015;69(9-10):399-405.
17. Gabriel Camelia. Compilation of the dielectric properties of body tissues at RF and microwave frequencies. KING'S COLL London (United Kingdom) Dept of Physics; 1996.
18. Fukunaga K, Watanabe S, Yamanaka Y, Asou H, Ishii Y, Satou K, Miyota Y. Dielectric properties of tissue equivalent liquids in practice. Tech. Rep. IEICE, No. EMCJ. 2002;44:13–17.
19. Faruque MRI, Husni NA, Hossain MI, Islam MT, Misran N. Effects of mobile phone radiation onto the human head with a variation of holding cheek and tilt positions. J. Appl. Res. Technol. 2014; 2(5):871–876.
20. Faruque MRI, Islam MT, Misran N. Effects of dielectric values and substrate materials on electromagnetic (EM) absorption in human head. Frequenz. 2012;66(3–4):79-83.
21. International Non-Ionizing Radiation Committee of the International Radiation Protection Association. Guidelines on limits on exposure to radio frequency electromagnetic fields in the frequency range from 100 kHz to 300 GHz. Health Physics. 1988;54(1):115-123.
22. IEEE standard for safety levels with respect to human exposure to radio frequency electromagnetic fields, 3 kHz to 300 GHz – Amendment 1: Specifies ceiling limits for induced and contact current, clarifies distinctions between localized exposure and spatial peak power density. IEEE Std C95.1a2010 (Amendment to IEEE Std C95.1-2005). 2010;C1–9.

Peer-review history:
The peer review history for this paper can be accessed here:
http://www.sdiarticle3.com/review-history/49566